

# Structural and magnetic characterization of norbornene–deuterated norbornene dicarboxylic acid diblock copolymers doped with iron oxide nanoparticles

Pinar Akcora<sup>a</sup>, Xin Zhang<sup>b</sup>, Bindhu Varughese<sup>c</sup>, Robert M. Briber<sup>b</sup>, Peter Kofinas<sup>a,\*</sup>

<sup>a</sup>Department of Chemical Engineering, University of Maryland, College Park, MD 20742-2111, USA

<sup>b</sup>Department of Materials Science and Engineering, University of Maryland, College Park, MD 20742, USA

<sup>c</sup>Department of Chemistry and Biochemistry, University of Maryland, College Park, MD 20742, USA

Received 18 January 2005; received in revised form 11 April 2005; accepted 11 April 2005

Available online 29 April 2005

## Abstract

A series of iron oxide doped norbornene (NOR)/deuterated norbornene dicarboxylic acid (NORCOOH) diblock copolymers were synthesized and characterized by X-ray photoelectron spectroscopy (XPS), small angle neutron scattering (SANS) and superconducting quantum interference device (SQUID) experiments.  $\gamma$ -Fe<sub>2</sub>O<sub>3</sub> nanoparticles were synthesized within the microdomains of diblock copolymers with volume fractions of NOR/NORCOOH 0.64/0.36, 0.50/0.50 and 0.40/0.60. A spherical nanoparticle morphology was displayed in the polymer with 0.64/0.36 volume fraction. Polymers with 0.50/0.50 and 0.40/0.60 volume fractions exhibited interconnected metal oxide nanostructures. The observed changes in the shape and peak positions of the small-angle neutron scattering profiles of polymers after metal doping were related to the scattering from the metal oxide particles and to the possible deformed morphologies due to the strong interparticle interactions between metal particles, which may influence the polymer microphase separation. The combined scattering from both polymer domains and magnetic particles was depicted in SANS profiles of metal oxide doped polymers.  $\gamma$ -Fe<sub>2</sub>O<sub>3</sub> containing block copolymers were superparamagnetic at room temperature. An increase in the blocking temperature ( $T_b$ ) of interconnected nanoparticles was observed and was related to the interparticle interactions, which depends on the average distance ( $d$ ) between particles and individual particle diameter ( $2R$ ). The sample with volume fraction of 0.4/0.6 have the lowest  $d/(2R)$  ratio and exhibit the highest  $T_b$  at 115 K.

© 2005 Elsevier Ltd. All rights reserved.

**Keywords:** Diblock copolymer; Iron oxide nanoparticles; Neutron scattering

## 1. Introduction

Magnetic nanoparticles are a subject of extensive research due to their interesting magnetic properties and technological applications such as ferrofluids, recording tapes, flexible high-density magnetic data storage, biomedical materials and catalysts [1,2]. The design and synthesis of magnetic nanoparticles with controlled size and uniform dispersion is an important subject in materials research [3,4]. Block copolymers which microphase separate into ordered morphologies such as lamellar, cylindrical and

spherical microdomains provide a self-assembled template for the synthesis of nanocomposites. These microdomains serve as nanoreactors within which a variety of nanoparticle clusters can be synthesized. In earlier studies, non-magnetic nanoparticles (Au, Ag, Pd, Pt, Cu) [5–9] and semiconductor nanoclusters (PbS, CdS, ZnS) [10–12] were synthesized within norbornene diblock copolymers. The synthesis and characterization of magnetic Fe<sub>2</sub>O<sub>3</sub> nanoparticles within a single block copolymer composition, NORCOOH<sub>30</sub> MTD<sub>300</sub>, (NORCOOH: 2-norbornene-5,6-dicarboxylic acid; MTD: methyltetracyclododecene) has been reported by Sohn et al. [13,3]. Synthesis of CoFe<sub>2</sub>O<sub>4</sub> nanoparticles within NOR<sub>400</sub>NORCOOH<sub>150</sub> (NOR: norbornene) polymer has also been reported for one diblock copolymer composition [14]. Both studies discuss the synthesis and morphology of magnetic oxide nanoparticles formed from templating at a single block copolymer composition. This

\* Corresponding author. Tel.: +1 301 405 7335; fax: +1 301 405 0523.

E-mail address: [kofinas@umd.edu](mailto:kofinas@umd.edu) (P. Kofinas).

URL: <http://www.glue.umd.edu/~kofinas>.

study reports on the effect of block copolymer composition variation on the templating, morphology, and magnetic properties of resultant magnetic nanoparticles formed within the diblock copolymer matrices. The norbornene dicarboxylic acid block of the block copolymer was deuterated to provide contrast for small-angle neutron scattering. The objective of this study is to analyze the effect of various copolymer morphologies on nanoparticle dispersion and magnetic properties by characterization of metal oxide doped polymers through X-ray photoelectron spectroscopy (XPS), transmission electron microscopy (TEM), small angle neutron scattering (SANS) and superconducting quantum interference device (SQUID) magnetometry.

## 2. Materials

Norbornene (99%) was purchased from Fischer Scientific and distilled over sodium under argon. Ethyl vinyl ether, dichloromethane ( $\text{CH}_2\text{Cl}_2$ ), deuterated fumaric-2,3- $d_2$  acid (98 at.%  $d$ ) and anhydrous ethanol were purchased from Aldrich.  $\text{CH}_2\text{Cl}_2$  was distilled over calcium hydride under argon. Bis(tricyclohexyl phosphine) benzylidene ruthenium(IV) dichloride (Grubbs's catalyst) was purchased from Strem Chemicals. All solvents, monomers and catalysts required for polymer synthesis were stored inside an MBraun Lab-Master100 glovebox.

## 3. Experimental

Deuterated 2-norbornene-5,6-dicarboxylic acid (NORCOOH) was synthesized through a Diels-Alder reaction. Cyclopentadiene was obtained from dicyclopentadiene cracking. Deuterated fumaric acid (5 g, 0.043 mole) was first dissolved in 250 ml ethanol. When the solution became clear, freshly cracked cyclopentadiene (2 molar eq.) was added to this solution. The reaction was complete in 12 h. Ethanol was stripped off, then the white precipitated solid was dissolved in pentane to remove the unreacted components. The white solid was dried at 50 °C oven for 3 days. The synthesis of 2-norbornene-5,6-dicarboxylic acid bis-trimethylsilyl ester has been reported in literature [15]. The same procedure was followed using deuterated norbornene dicarboxylic acid to synthesize deuterated norbornene dicarboxylic acid bis-trimethylsilyl ester.

Ring-opening polymerization (ROMP) has been used to synthesize function-alized block copolymers with well-defined architectures and narrow molecular weight distributions. In our study, deuterated diblock copolymers were synthesized by sequential polymerization of norbornene (NOR) followed by deuterated norbornene dicarboxylic acid (NORCOOH). The first generation Grubbs's catalyst was used in the polymerization of norbornene homopolymer. Synthesis was conducted according to literature

procedures [16]. The diblock copolymer consists of  $\text{NOR}_m/\text{deuterated-NORCOOH}_n$  where  $m$  and  $n$  are the repeating units (Fig. 1).  $m$  and  $n$  values were determined through measurement of refractive index change by concentration ( $dn/dc$ ) and gel permeation chromatography–light scattering analysis. The yields of the deuterated diblock copolymers were determined to be 96% for  $\text{NOR}_{360}/\text{NORCOOH}_{120}$ ; 83% for  $\text{NOR}_{320}/\text{NORCOOH}_{190}$  and 91% for  $\text{NOR}_{290}/\text{NORCOOH}_{260}$ .

The carboxylic acid groups of norbornene–deuterated norbornene dicarboxylic acid diblock copolymer solution in tetrahydrofuran (THF) (3 wt%) were associated with the required amount of iron salts in THF (ion exchange reaction between  $\text{FeCl}_3$  and  $\text{NORCOOH}$  requires a 1:1  $\text{Fe}^{+3}:\text{COO}^{-1}$  molar ratio) at room temperature overnight. Polymers containing the iron salts were static solution cast on teflon covered aluminum cups to make thin films. The solvent was slowly evaporated and the films were dried for 6 days. The films were soaked in 2 M NaOH solutions to produce  $\text{Fe}_2\text{O}_3$  particles and then washed with water. Elemental analysis of Fe-doped polymers after the washing step indicated that the iron amount in the samples had decreased after the washing step (Table 1), which indicated that some Fe ions were not associated with the carboxylic acid groups during iron doping.

## 4. Characterization techniques

Molecular weight distributions and absolute molecular weights were measured by gel permeation chromatography/light scattering (GPC/LS) using a Wyatt Technology Mini-DAWN light scattering detector, a Waters 2410 RI detector and a Waters 515 pump and a Rheodyne 7125i injector with a 200  $\mu\text{L}$  loop. The mobile phase was THF with 1 ml/min flow rate. Waters styragel  $10^4$ ,  $10^5$  and  $10^6$  Å columns were used for these measurements.

The morphologies of the metal oxide doped polymers and metal oxide particle sizes were examined by TEM (Hitachi H-600, operated at 100 keV). TEM samples were prepared by ultramicrotoming using a diamond knife.

Magnetic characterization was performed by superconducting quantum interference device measurements. The temperature dependence of the magnetization was determined by zero field-cooled (ZFC) and field-cooled

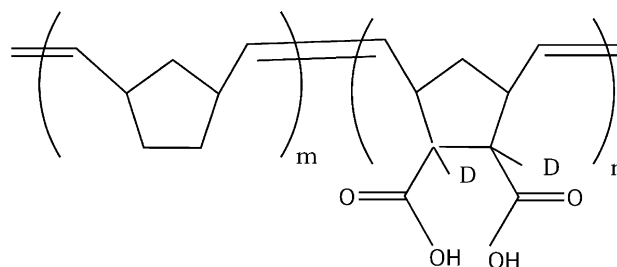


Fig. 1.  $[\text{NOR}]_m[\text{NORCOOH}]_n$  chemical structure.

Table 1  
Fe amounts (wt%) in diblock copolymer samples before and after washing

Sample ( <i>m/n</i> )	wt% Fe before washing	wt% Fe after washing
360/120	7.4	6
320/190	9.4	7
290/260	11.7	10

(FC) measurements. The ZFC curve was obtained by cooling down to 5 K at zero field and then measuring the magnetization under a 200 Oe applied magnetic field. The magnetization was measured during heating from 5 K to room temperature at 5 K intervals. The FC curve was similarly obtained except that this time the sample was cooled while applying a 200 Oe magnetic field.

Small angle neutron scattering experiments were carried out at the Center for Neutron Research at the National Institute of Standards and Technology (NCNR) on the 8-m NG1 [17] instrument. 10 Å wavelength neutrons were used. The sample to detector distance was set to 3.84 cm and the detector angle was 3.5°.

X-ray photoelectron spectroscopic measurements were performed using a Kratos Axis 165 spectrometer at a vacuum of  $4 \times 10^{-10}$  Torr with non-monochromatic Mg K $_{\alpha}$  radiation. All measurements were done in electrostatic mode, with a step size of 0.1 eV and sweep time of 60 s. All individual region spectra are recorded in the fixed analyzer transmission analyzer mode with pass energy of 20 eV.

## 5. Results and discussion

The microstructure of iron oxide particles was determined by X-ray photoelectron spectroscopy (XPS). After subtraction of a linear background, all spectra are fitted using 60% Gaussian/40% Lorentzian peaks, taking the minimum number of peaks consistent with the best fit. The important parameters in the fitting process are peak position, full width at half maximum, intensity and the Gaussian fraction. The high resolution Fe 2p spectrum of the sample is shown in Fig. 2. The main Fe (2p 3/2) structure is a broad peak with a full width at half maximum of about 3.8 eV. Since the asymmetric structure is clear in this peak envelope, it has been resolved to various components as described by Zetaruk et al. [20]. The peak envelope is well fit by a series of peaks of decreasing intensity constrained to similar width and shape. Analysis of the two main peaks in the Fe (2p 3/2) envelope has shown that spin orbit splitting is 1.0 eV, which matches exactly the value reported for  $\gamma$ -Fe $_2$ O $_3$  in the literature [20]. Earlier calculations and studies have shown that both  $\alpha$ -Fe $_2$ O $_3$  and  $\gamma$ -Fe $_2$ O $_3$  yield similar intensity distributions for the Fe (2p 3/2) peak envelope. The only change is the multiplet splitting distribution within each peak. The spin orbit splitting is 1.2 eV for  $\alpha$ -Fe $_2$ O $_3$  where as  $\gamma$ -Fe $_2$ O $_3$  has a splitting of 0.2 eV less than  $\alpha$ -Fe $_2$ O $_3$ . We therefore conclude from the

XPS data that the iron oxide is present as  $\gamma$ -Fe $_2$ O $_3$ . The small peak between 708 and 710 eV indicates the presence of Fe $_3$ O $_4$  in the peak envelope after the peak fitting.

The molecular weights of the first and second blocks are analyzed using GPC/LS. The measurement of the molecular weights of both blocks, allows the number of monomer repeating units in each constituent blocks to be computed. Actual molecular weights, block ratios, polymer compositions and molecular weight distributions were determined from the analysis of GPC data as shown in Table 2.

In this study, the NORCOOH block was deuterated to provide contrast between the two blocks for SANS. The neutron scattering data for each sample plotted as intensity (*I*) versus scattering vector (*Q*) is shown in Fig. 3. Peak positions observed in the SANS data shifted to higher *Q* values with increasing NOR content, which indicated increasing separation of block copolymer domains and potential changes in morphology. The domain spacing, which is the average center-to-center distance of the microphase separated diblock copolymer domains, was calculated from the peak positions maxima ( $d = 2\pi/Q$ ) and is shown in Table 3.

SANS experiments with metal oxide doped polymers were performed using the same experimental configurations as for the undoped polymer samples. A change in the shape of the scattering profiles of metal oxide doped polymers (Fig. 4) were observed compared to that of undoped polymers. These profiles represent the combined scattering from both the polymer domains and magnetic particles at room temperature. Spin dependent magnetic scattering cannot be observed above the ordering temperature, which is around 10 K for these systems. Magnetic and nuclear scattering contributions can in general be separated by conducting scattering experiments below the ordering temperature [18] or by performing experiments with polarized neutrons [19]. In our study, only the nuclear scattering from Fe $_2$ O $_3$  nanoparticles contributed to the scattering from the polymer domains. The domain spacing obtained by the  $Q_{\max}$  values of the SANS curves of the metal oxide doped polymers refers to scattering contributions of the underlying microphase separated polymer domains, combined with any scattering from the metal oxide nanoparticles. This spacing was consistently smaller than the spacing obtained from the SANS profiles of the undoped block copolymers. The domain spacings calculated

Table 2  
Measured molecular weights, compositions, PDI and volume fractions ( $\phi$ ) of a series of norbornene diblock copolymers

Total polymer $M_w$ (g/mole)	NOR/NORCOOH polymer composition	PDI ( $\bar{M}_w/\bar{M}_n$ )	$\phi_{\text{NOR/NORCOOH}}$
55,941	360/120	1.67	0.64/0.36
65,074	320/190	1.24	0.50/0.50
75,146	290/260	1.36	0.40/0.60

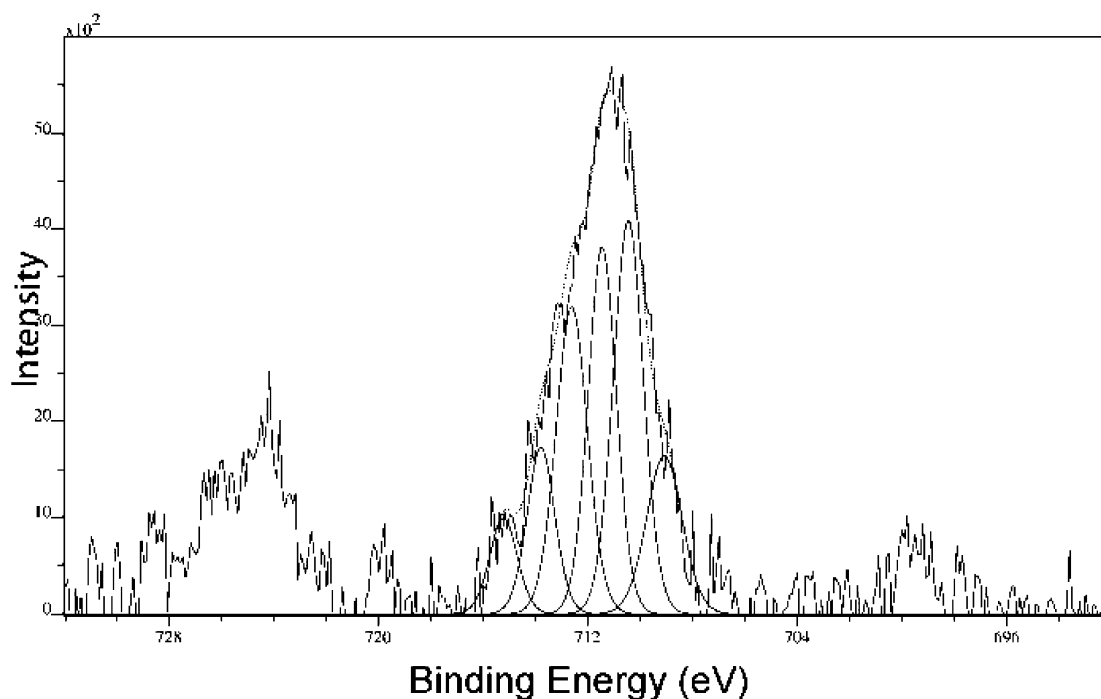


Fig. 2. XPS spectra of  $\gamma$ -Fe<sub>2</sub>O<sub>3</sub> nanoparticles in NOR<sub>360</sub>NORCOOH<sub>120</sub>.

from the peak positions of undoped and metal oxide doped samples are shown in Table 3 for comparison.

Transmission electron microscopy indicated that the diblock copolymers with Fe<sub>2</sub>O<sub>3</sub> exhibited spherical and interconnected morphologies. The sample synthesized with constituent block volume fraction ratio  $\phi_{\text{NOR}/\text{NORCOOH}} = 0.64/0.36$  had a disordered spherical morphology with average particle size of 10.4 nm as shown in Fig. 5. The

spacing between the magnetic nanoparticles of this sample was determined by 2-dimensional Fourier transform (FFT) analysis of the TEM image. The spacing of the metal oxide particles, 62 nm, was found to be close to the domain spacing of 53 nm obtained by SANS. The comparison of  $I$  versus  $Q$  plots is presented in Fig. 6.

The metal oxide doped polymer samples with 0.50/0.50 and 0.40/0.60 volume fraction ratios exhibited

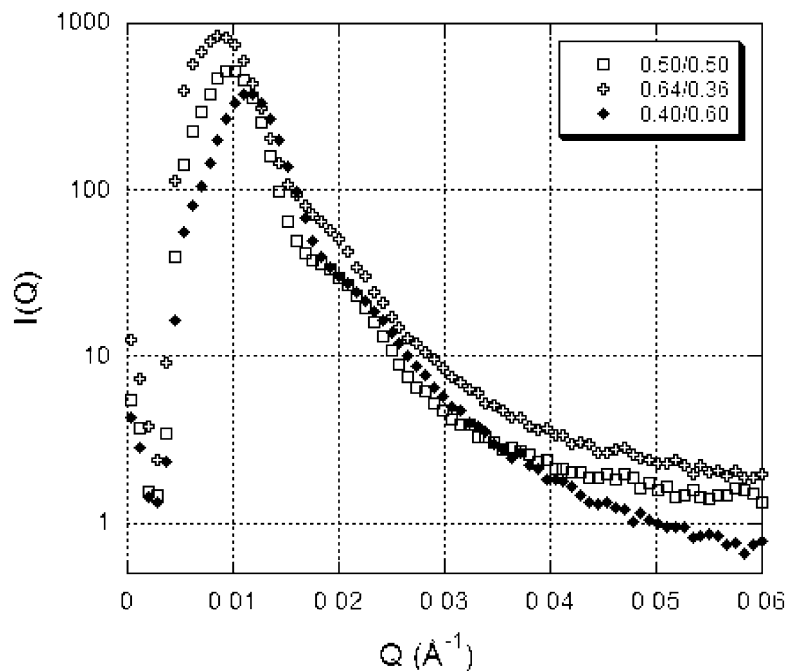


Fig. 3. SANS profiles of the series of norbornene/deuterated norbornene dicarboxylic acid block copolymers.

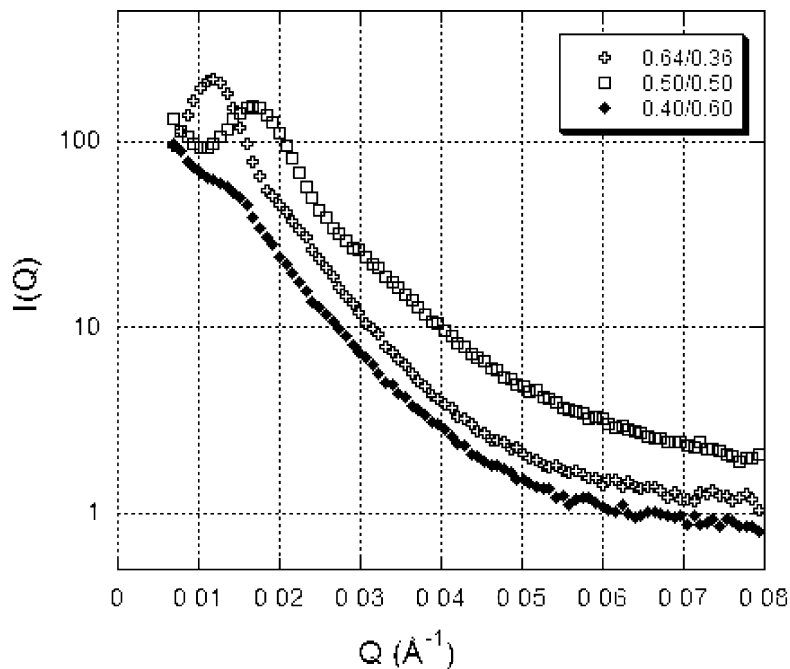


Fig. 4. SANS profiles of the series of norbornene/deuterated norbornene dicarboxylic acid block copolymers with iron oxide nanoparticles.

Table 3

*d*-Spacings for series of undoped and doped diblock copolymers with Fe<sub>2</sub>O<sub>3</sub>

$\phi_{\text{NOR/NORCOOH}}$	$d_{\text{undoped}} = 2\pi/Q$ , (Å)	$d_{\text{doped}}$ , (Å)
0.64/0.36	730	530
0.50/0.50	670	375
0.40/0.60	530	439

interconnected morphologies, as shown in Figs. 7 and 8. The average particle size was found to be 10.7 and 16 nm for the sample with volume fractions of 0.50/0.50 and 0.40/0.60. The metal-doped samples exhibit morphologies, which were different than the expected morphologies from the copolymer compositions. The reason for the disordered morphologies can be possible non-equilibrium conditions occurring during the solvent casting and the interparticle interactions affecting the microphase separation and desired morphology. For example, an interconnected morphology was observed from the diblock copolymer with 50/50 volume fraction ratio instead of the expected lamellar morphology. FFT of the TEM images did not give a peak for these samples because TEM images do not present enough order in the particular areas.

## 6. Magnetic characterization of $\gamma$ -Fe<sub>2</sub>O<sub>3</sub> doped diblock copolymers

All the ZFC curves shown in Fig. 9 represent broad distributions of particle size and blocking temperatures. The blocking temperatures were calculated from the maxima of the ZFC curves.

The change in blocking temperature is related to the

particle size and relaxation time distributions of the particles. The temperature  $T_s$  where the ZFC and FC curves meet, corresponds to the blocking of the largest particles.  $T_s - T_b$  is a measure of the width of the energy barrier and thus relates to the particle size distribution. Both temperatures,  $T_b$  and  $T_s$  are given in Table 4. In our study, it was

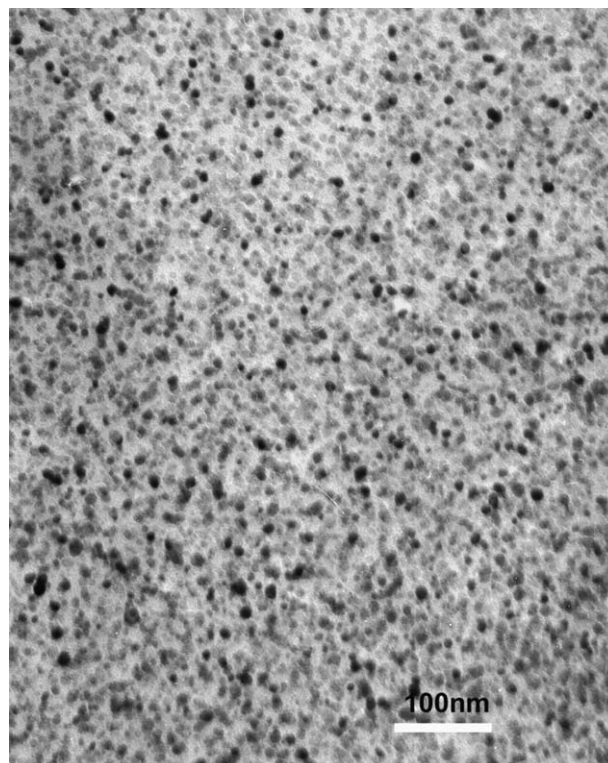


Fig. 5. TEM image of 0.64/0.36 polymer doped with Fe<sub>2</sub>O<sub>3</sub> nanoparticles.

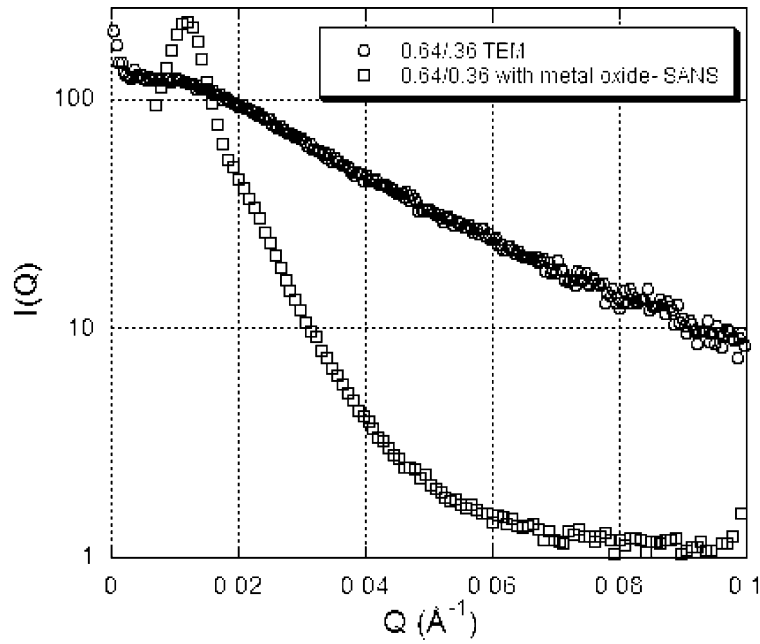


Fig. 6. Comparison of  $d$ -spacings of metal oxide doped polymer 0.64/0.36 from SANS and TEM. The  $d$ -spacing between metal oxide nanoparticles and metal oxide doped polymer domains are found as 62 and 53 nm, respectively.

found that the blocking temperature increased with decreasing polymer domain spacing. This behavior is probably related to interparticle interactions. Magnetic interactions between superparamagnetic particles may influence the relaxation time and anisotropy energy. The effect of particle interactions on the dynamic and static properties of  $\gamma$ -Fe<sub>2</sub>O<sub>3</sub> nanoparticles dispersed in polyvinyl

alcohol homopolymer has been studied by ac susceptibility and Mossbauer spectroscopy measurements in an earlier study [21]. Thermal variation of the relaxation time has been observed for samples with different particle spacings. As the ratio of center-to-center distance between particles ( $d$ ) to average particle diameter ( $2R$ ),  $d/2R$ , varied from 3.9 to 1.6, the energy barrier due to interactions ( $E_B(0)$ )

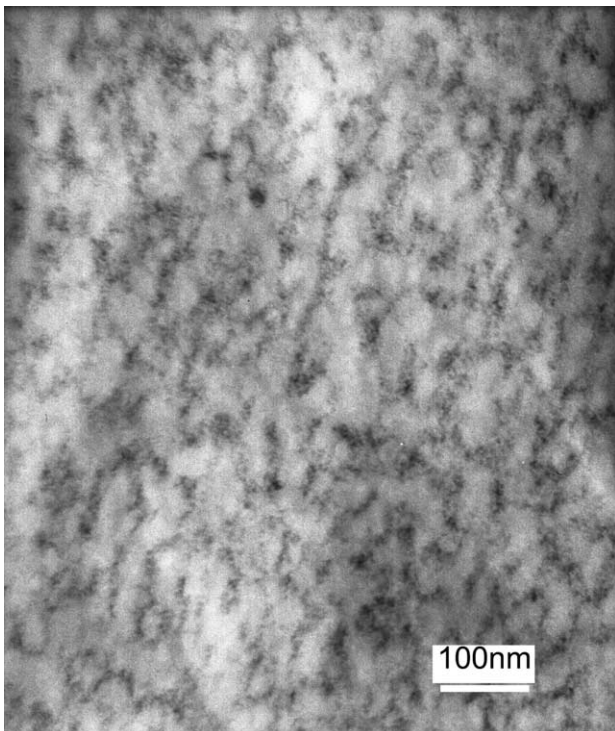


Fig. 7. TEM image of 0.50/0.50 polymer doped with Fe<sub>2</sub>O<sub>3</sub> nanoparticles.

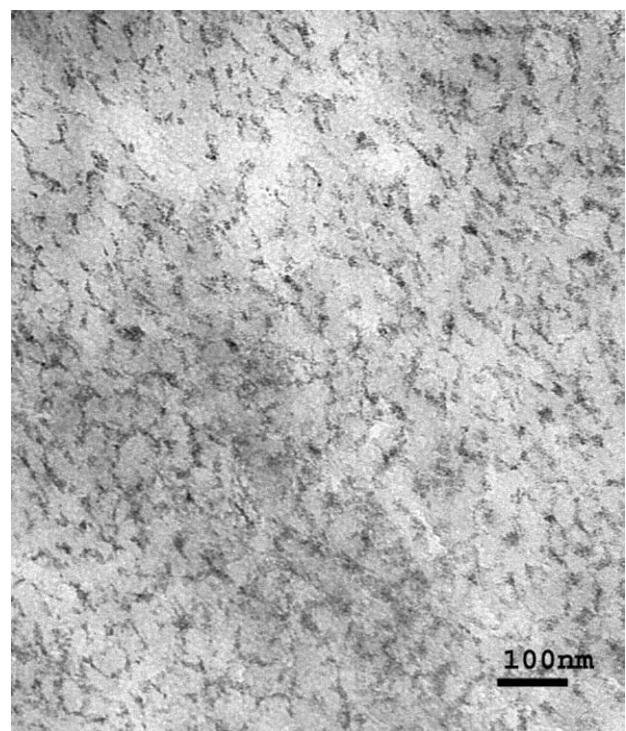


Fig. 8. TEM image of 0.40/0.60 polymer doped with Fe<sub>2</sub>O<sub>3</sub> nanoparticles.

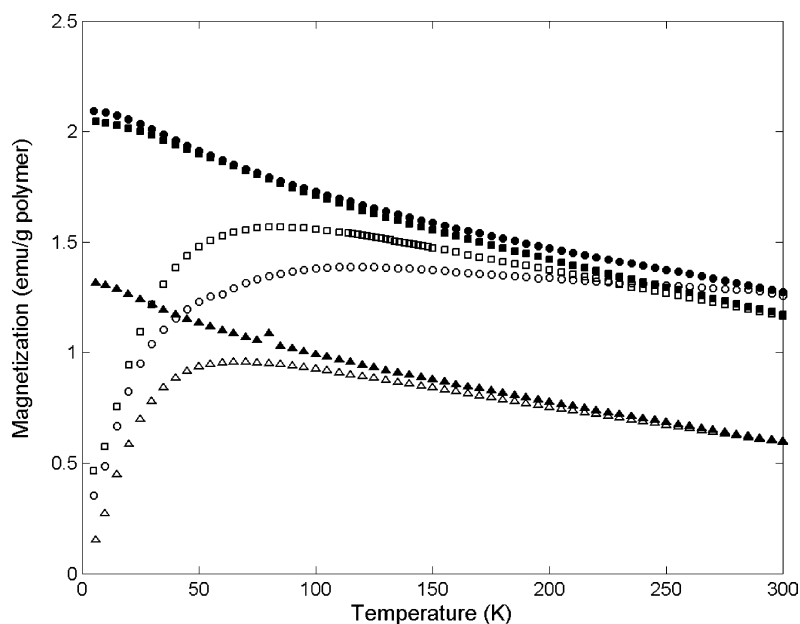


Fig. 9. ZFC–FC magnetization curves as a function of temperature with 200 Oe applied magnetic field for sample 0.64/0.36 ( $\Delta$ ), 0.50/0.50 ( $\square$ ) and 0.40/0.60 ( $\circ$ ). Filled and unfilled symbols represent FC and ZFC curves, respectively.

increased from 38 to 275 and resulted in higher blocking temperatures [22,23]. Dormann et al. showed that the sample with the smallest particle spacing had the highest  $T_b$  within a series of samples with the same particle size. They found that the sample with  $d/2R \sim 4.7$  (which had the largest spacing) was consistent with non-interacting particles. The effect of relaxation of the particle moment on interparticle interaction energy was accounted for using a statistical calculation of the energy barrier. For our samples, the corresponding  $d/2R$  ratios were determined to be 5.09, 3.50 and 2.7 for 0.64/0.36, 0.50/0.50, 0.40/0.60 samples, respectively.  $d$  values for the metal oxide doped polymers were determined from the SANS data and  $R$  was determined

Table 4

Blocking temperature variation with block copolymer composition, obtained from ZFC measurements with SQUID

Polymer volume fractions	$T_b$ , (K)	$T_s$ , (K)	$d/2R$
0.64/0.36	70	200	5.09
0.50/0.50	85	250	3.50
0.40/0.60	115	290	2.29

Table 5

Magnetization values at 50 kOe for varying block copolymer compositions at 10 and 300 K

Polymer volume fractions	emu/g polymer		emu/g $\gamma$ -Fe <sub>2</sub> O <sub>3</sub>	
	10 K	300 K	10 K	300 K
0.64/0.36	7	5	81	58
0.50/0.50	8	7	80	70
0.40/0.60	14	11	97	76

by TEM. These  $(d)_{\text{SANS}}/(2R)_{\text{TEM}}$  ratios were similar in magnitude to the values found by Dormann et al. Therefore, the observed increase in  $T_b$  from 70 to 115 K is probably due to the decreasing ratio  $d/2R$  and the concomitant increase in interparticle interactions.

The magnetizations at an applied field of 50 kOe per gram of polymer and per gram of Fe<sub>2</sub>O<sub>3</sub> at different temperatures are presented in Table 5. Magnetization values increased with increasing amount of Fe<sub>2</sub>O<sub>3</sub> in the diblock copolymers. The thermal dependence of the magnetization was observed at 10, 50 and 300 K to be between  $-0.5$  and  $0.5$  kOe. Magnetic measurements revealed that the samples were superparamagnetic at room temperature. Below their blocking temperatures, hysteresis loops were observed for all samples. Fig. 10 presents the magnetization profiles as a function of field for sample with volume fraction of 0.40/0.60 at 10, 50 and 300 K. Samples 0.64/0.36, 0.50/0.50 and 0.40/0.60 became ferrimagnetic at 10 K. Magnetization profiles for all samples between  $-50$  and  $+50$  kOe at 10 K are presented in Fig. 11. The magnetization of sample 0.40/0.60 with the highest metal oxide content remained unsaturated at the highest field 50 kOe, at 10 K.

## 7. Conclusions

Spherical and interconnected morphologies of  $\gamma$ -Fe<sub>2</sub>O<sub>3</sub> nanoparticles were synthesized within different block copolymer compositions and characterized in TEM. FFT analysis of the TEM image from the 0.64/0.36 sample showed that the spacing between the metal oxide particles in the TEM image (62 nm) was consistent with the polymer spacing of 53 nm measured by SANS. Similar spacings

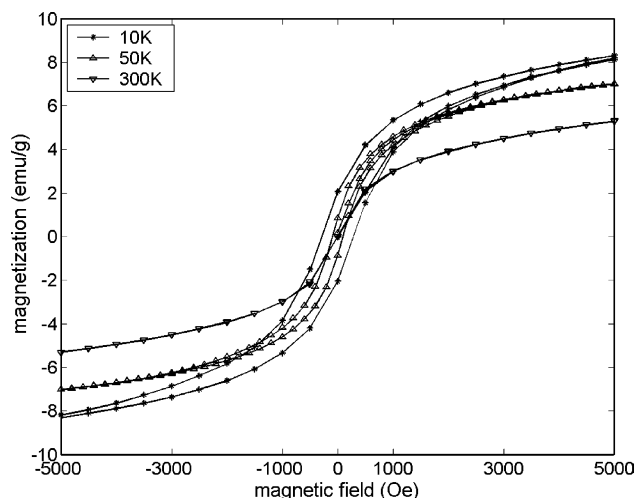


Fig. 10. Magnetization versus applied magnetic field for the block copolymer with volume fraction of 0.40/0.60 containing  $\text{Fe}_2\text{O}_3$  nanoparticles at 10, 50 and 300 K.

between polymer domains and metal oxide particles indicate the control of the dispersion of metal oxide particles within the diblock copolymer template.

The SANS profiles revealed that domain spacings decreased after metal doping. Scattering from magnetic particles can change the observed profiles if the iron particles are not distributed uniformly within the polymer nanodomains. Therefore, the change in domain spacing is due to the non-uniform distribution of magnetic particles or to the strong interparticle interactions, which may influence the block copolymer microphase separation. An increase in blocking temperatures indicates particle interactions that change with nanoparticle size and domain distance. Sample (0.40/0.60) with the highest blocking temperature of 115 K exhibited an interconnected morphology. All metal oxide doped samples were superparamagnetic at 300 K and became ferrimagnetic at 10 K.

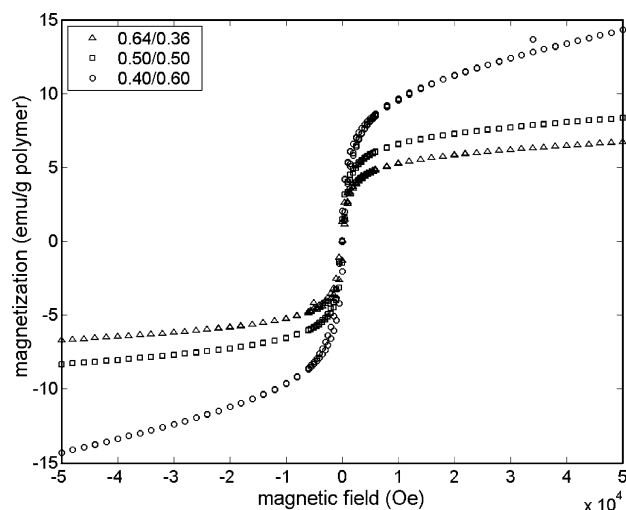


Fig. 11. Magnetization versus applied magnetic field for all samples at 10 K.

The room temperature neutron scattering data does not contain spin-dependent magnetic scattering from  $\text{Fe}_2\text{O}_3$  particles because all spins are disordered at this temperature. In future studies, small-angle neutron scattering experiments are planned above and below the ordering temperature to better understand structural and magnetic ordering and spin-pair correlations of iron oxide nanoparticles within the self-assembled diblock copolymer domains.

## Acknowledgements

This material is based upon work supported by the National Science Foundation Grant # CTS-0347319. We acknowledge H. Balci for his help in using the SQUID instrument at Center for Superconductivity Research, Department of Physics at University of Maryland. We acknowledge the support of the National Institute of Standards and Technology, US Department of Commerce, in providing the neutron research facilities used in this work. This work utilized facilities supported in part by the National Science Foundation under Agreement # DMR-9986442.

## References

- [1] Kodama RH. *J Magn Magn Mater* 1999;200:359.
- [2] Predoi D, Kuncser V, Tronc E, Nogues M, Russo U, Principi G, et al. *J Phys Condens Matter* 2003;15:1797.
- [3] Sohn BH, Cohen RE, Papaefthymiou GC. *J Magn Magn Mater* 1998; 182:216.
- [4] de Caro D, Ely TO, Mari A, Chaudret B, Snoeck E, Respaud M, et al. *Chem Mater* 1996;8:1987.
- [5] Clay RT, Cohen RE. *Supramol Sci* 1995;2:183.
- [6] Ciebien JF, Clay RT, Sohn BH, Cohen RE. *New J Chem* 1998;7:685.
- [7] Clay RT, Cohen RE. *New J Chem* 1998;7:745.
- [8] Boontongkong Y, Cohen RE, Rubner MF. *Chem Mater* 2000;12:1628.
- [9] Chan YC, Schrock RR, Cohen RE. *Chem Mater* 1992;4:24.
- [10] Kane RS, Cohen RE, Silbey R. *Chem Mater* 1996;8:1919.
- [11] Yue J, Cohen RE. *Supramol Sci* 1994;1:117.
- [12] Cummins CC, Schrock RR, Cohen RE. *Chem Mater* 1992;4:27.
- [13] Sohn BH, Cohen RE. *Chem Mater* 1997;9:264.
- [14] Ahmed SR, Ogale SB, Kofinas P. *IEEE Trans Magn* 2003;39:2198.
- [15] Royappa AT, Saunders RS, Rubner MF, Cohen RE. *Langmuir* 1998; 14:6207.
- [16] Ahmed RS, Kofinas P. *Macromolecules* 2002;35:3338.
- [17] National Institute of Standards and Technology Center for Neutron Research. NG3 and NG7 30-meter SANS instruments data acquisition manual; June 2002.
- [18] Seehra MS, Babu VS, Manivannan A, Lynn JW. *Phys Rev B* 2000;61: 3513.
- [19] Spizzo F, Angeli E, Bisero D, Da Re A, Ronconi F, Vavassori P, et al. *J Appl Cryst* 2003;36:826.
- [20] McIntyre NS, Zetaruk DG. *Anal Chem* 1977;49:1521.
- [21] Dormann JL, Bessais L, Fiorani D. *J Phys C Solid State Phys* 1988;21: 2015.
- [22] Dormann JL, Spinu L, Tronc E, Jolivet JP, Lucari F, D'Orazio F, et al. *J Magn Magn Mater* 1998;183:L255.
- [23] Dormann JL, Fiorani D, Cherkaoui R, Tronc E, Lucari F, D'Orazio F, et al. *J Magn Magn Mater* 1999;203:23.